Micromachined Electrodes for High Density Neural Stimulation Systems

Andy Hung[1], David Zhou[3], Robert Greenberg[3], and Jack W. Judy[2]

[1]Biomedical Engineering IDP and [2]Electrical Engineering Dept.,
University of California, 420 Westwood Plaza, Los Angeles, CA 90094, USA

[3]Second Sight, LLC, 28460 Avenue Stanford, Suite 200, Valencia, CA 91355, USA

***Abstract*—High-resolution retinal prosthetic systems require high-density stimulation electrodes to restore the vision of blind patients suffering from retinitis pigmentosa and macular degeneration. Micromachining the surface of electrodes to obtain high aspect ratio features can tremendously increase the effective area of the electrode. A unique process has been developed to obtain high aspect ratio structures by plating on the sidewall of recently developed and insufficiently rinsed resist. A quadrupling of the effective area of the electrode surface has been achieved with modest micromachining and should translate into a similar improvement in visual resolution.**

I. Introduction

Micromachining has long been used to produce neural-electronic interfaces for recording neural activity of individual cells and clusters of cells with planar electrode arrays [1-2] and probe arrays [3-4]. Recently, new applications that require the stimulation of neural tissues are pushing the performance limits of conventionally produced microelectrode arrays. One good example is the development of a visual prosthesis. Blind patients with retinitis pigmentosa and macular degeneration suffer from the degradation of photoreceptors in the retina. However, as indicated by clinical studies, visual percepts can still be induced by direct electrical stimulation of the remaining ganglion or bipolar neural layers of the retina [5-6] (Figure 1).

Internationally, several efforts are under way to construct a full visual prosthetic system. The epi-retinal approach, shown in Figure 2, is being developed by Second Sight, LLC [7]. A camera mounted on a pair of glasses captures images, which are then processed by a computer to reduce and prepare the information for the prosthetic device. The visual-signal information is then sent via RF telemetry to an integrated circuit implanted inside the eye, which then decodes the information, and modulates the stimulation electrodes.

One technological challenge in the development of a visual prosthesis is the stimulation resolution of the electrode array. To increase resolution, the size of each electrode or 'pixel' needs to be reduced. However, the minimum electrode size is dictated by the charge necessary to induce retinal stimulation and the charge-injection limit of the electrode material. From acute clinical studies performed to date, the total charge required to illicit a visual percept is approximately 0.5 mA · 2 msec = 1 μC [6]. For a fixed charge the charge density increases as electrode size is reduced. If the charge density exceeds the reversible charge injection limit of the electrode material, undesirable and irreversible electrochemical reactions will occur. For platinum electrodes, which have an often-quoted injection limit of 100 μC/cm^2, the corresponding minimum electrode size is 1 mm^2 – much larger than the retinal cellular resolution of 10 μm^2 [8]. If the stimulated area of the retina were approximately 5×5 mm^2, planar electrodes would only enable an electrode array with a resolution of 5×5.

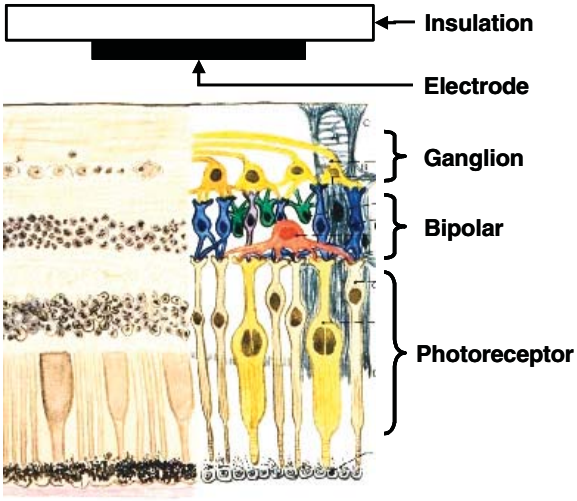

Figure 1. Cross section of the retina and an electrode used to stimulate the ganglion and bipolar cells to illicit visual perceptions in blind patients suffering from retinitis pigmentosa and macular degeneration.

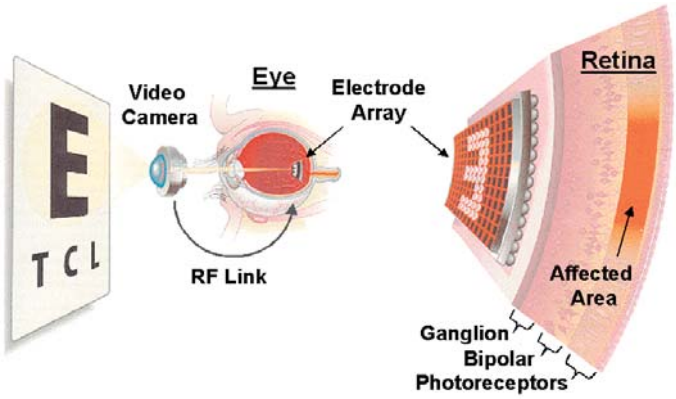

Figure 2. Retinal prosthetic system [7].

To increase the charge injection limit per electrode, one solution is to increase the surface area of the stimulation electrode, by using a process that forms platinum black by electroplating. While platinum black is a simple process that yields a large area increase, the approach is unreliable for long-term implantations because its flimsy dendritic structures are not mechanically robust and they would quickly dissolve and thereby loose its effectiveness. Our work reported here increases the surface area of electrodes by creating a robust array of high aspect ratio microstructures.

The surface area of an electrode is a strong function of its geometry (Fig. 3). The area of a flat electrode A_{flat} can be increased by a factor of 2 if formed into a hemispherical bump. It is possible to increase the surface further by raising the height-to-width aspect ratio. If a flat electrode surface of area $A_{flat} = (2w)^2$ is reshaped to include posts with a height h and width w, the total electrode surface area becomes $A_{post} = (2w)^2 + 4w \cdot h$. Thus in terms of the post aspect ratio h/w, the surface area is increased by a factor of $A_{post} = A_{flat} \cdot (1+h/w)$. Since aspect ratios of 2 or more are easily achieved with micromachining, one should expect to be able to obtain an area increase of a factor of 3 or more.

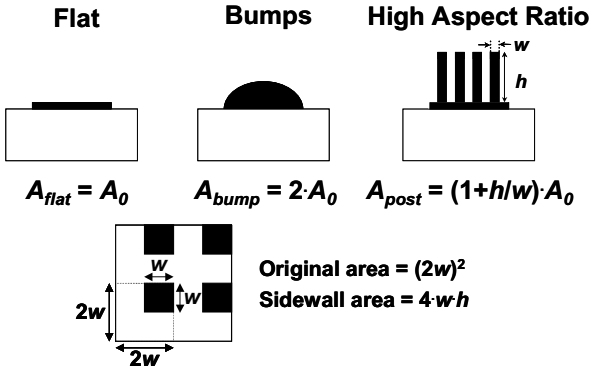

Figure 3. Cross sections of different micromachined electrodes and the corresponding increase in electrode surface area.

A. Fabrication

Both flat and high aspect ratio electrode arrays were produced using a batch-fabrication process, as shown in Fig. 4, which combines polyimide, titanium, and either platinum or gold. In addition, electrode arrays were constructed on both rigid and flexible substrates. Polyimide is used as the mechanical supporting material and electrical isolation for the flexible electrodes because of its excellent mechanical resiliency and chemical resistance. Since key aspects of the fabrication process for the rigid and flexible arrays are largely the same, the process described in detail here will be for the flexible arrays. Differences for the fabrication of the rigid arrays will be noted but not described in detail.

The fabrication process begins with a silicon wafer, which simply acts as a passive substrate. A 5-µm-thick film of polyimide is deposited to form the lower insulator and base of the mechanical support for the flexible array. For the rigid electrode arrays, a 500-nm-thick film of silicon dioxide is used as the lower insulator.

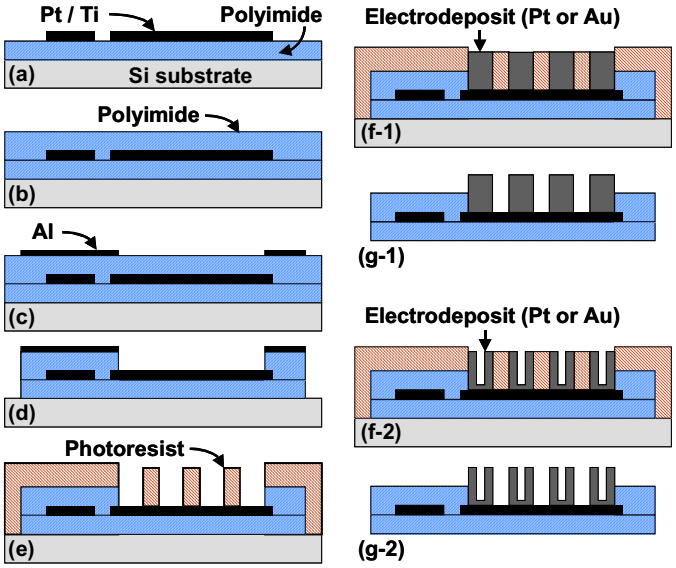

Figure 4. Batch-fabrication process used to construct the flexible arrays of micromachined electrodes, both with arrays of solid posts (f1-g1) and hollow posts (f2-g2).

The electrical base of the electrode array and the interconnect is formed by a 100-nm-thick film of titanium and a 100-nm-thick film of platinum deposited by e-beam evaporation. A lift-off process that uses STR 1045 photoresist (Shipley) and an acetone soak was used to pattern the metals films (Fig. 4a).

A second layer of polyimide is spun on to a thickness of 5 µm and then hard baked at 350ºC to form a structure in which the Ti/Pt film is sandwiched between two insulating polyimide layers (Fig. 4b).

The upper polyimide layer must be patterned to expose the electrode site. To accomplish this, we first deposit and pattern an aluminum etch mask and then remove all unprotected polyimide in an oxygen plasma etch (Oxford Plasmalab) (Fig. 4c-d). This step exposes the platinum electrode surface and mechanically separates the individual electrode arrays.

A 25-µm-thick layer of photoresist (Shipley SJR 5740) is used to define openings for the subsequent electroplating of the high aspect ratio microstructures made of Pt or Au (Fig. 4e-f). We are able to plate platinum and obtain smooth structures with good adhesion to a Pt plating seed layer. However, if the thickness of the plated Pt exceeds 0.5 µm, the high stress in the plated platinum can cause the film to delaminate from the Pt seed layer or lift up the seed layer from the lower polyimide film. We are also able to plate gold microstructures with no observed stress and did not delaminate. Once the high aspect ratio structures have been plated, the photoresist-plating mask is removed and the electrodes are electrochemically tested (Fig. 4g).

Initially the electrode surfaces consisted of arrays of microposts or the inverse, a micromesh. However, due to the stress in the electrodeposit, the much larger structures formed for the mesh electrode geometry were found to be impractical for platinum. Figure 5 shows a close-up of the electrode surface form with an array of microposts.

Occasionally during the plating process we observed an unexpected yet beneficial outcome. Specifically, in some instances, electrodeposition occurred on the sidewalls of the photoresist plating mold. The result is that instead of a micropost we obtained a *hollow* micropost (Fig. 6), which clearly has an even larger surface area. As shown in Fig. 3, the increase in electrode surface area for the hollow microposts over a flat electrode is a factor of $A_{post} = A_{flat} \cdot (1 + 2(h/w))$.

During the normal developing process, the KOH-based developer removes the exposed regions of the photoresist (Shipley SJR 5740) and then is rinsed away thoroughly. If the rinsing procedure is inadequate, the KOH-based developer is not sufficiently diluted, particularly from the sidewalls of the exposed resist, and therefore the sidewall conductivity is high enough to act as a seed layer during electrodeposition. In fact, a cross section of a hollow cylindrical micropost reveals that indeed the thickness of the plated material on the base of the hollow micropost is the same as that grown on the sidewalls of the exposed resist. It is also noteworthy that only the sidewalls of the resist became plated and not the top surface of the resist. A systematic study of the impact of the rinsing process on sidewall plating showed that when a developed sample is soaked in stagnant water for less than 10 minutes, plating will occur on the resist side walls. Longer soaks result in the expect results (i.e., flat plating of the electrode surface up through the plating mold to result in a solid micropost). The sidewall plating process has been found to be reproducible also for the electrodeposition of platinum, gold, and even nickel.

II. ELECTROCHEMISTRY RESULTS

To characterize the electrochemical dependence of electrode area for the flat and micromachined structures, an impedance analyzer is used to measure the current induced by the application of a small voltage fluctuation (e.g., 5 mV) over a wide range of frequencies (e.g., 1 to 100 kHz) as show in Figure 8. Typically, an electrode surface can be modeled with a capacitive C_e and resistive R_e element in parallel and another resistance R_s in series with (Figure 8) [9]. The capacitance of the electrode C_e corresponds to the fast charge build up across the electrode-electrolyte interface when voltage is applied. The electrode-electrolyte resistance R_e describes the lower faradaic conductance of charge transfer by means of chemical reaction between solution and the electrode metal. The series resistance R_s represents the resistance of the solution.

The C_e and R_e values typically vary widely with voltage, time, and concentration, and are challenging to model precisely. However, because our experimental setup employs small ac voltage fluctuations, R_e, C_e, and R_s can be approximated by simple linear values over the small voltage range. Since C_e is proportional to surface area ($C_e = \varepsilon_0 \cdot A/d$) and R_s is inversely dependent on area ($R_e = \rho \cdot l/A$), the resulting parallel conductance is also directly proportional to surface area ($j\omega C_e \parallel 1/R_e \propto A$).

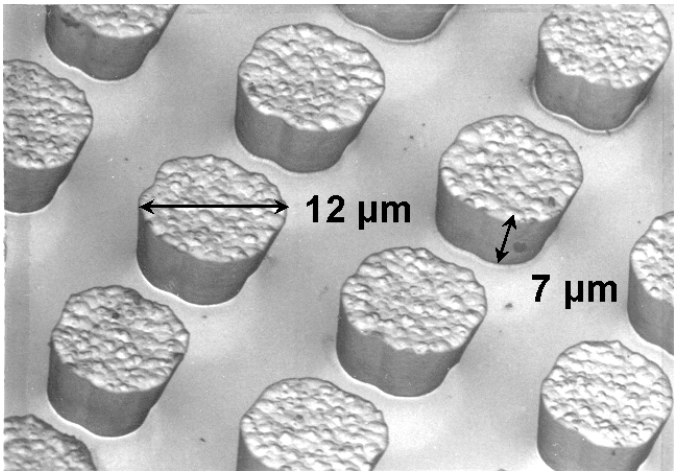

Figure 5. SEM image of the micromachined electrode surface.

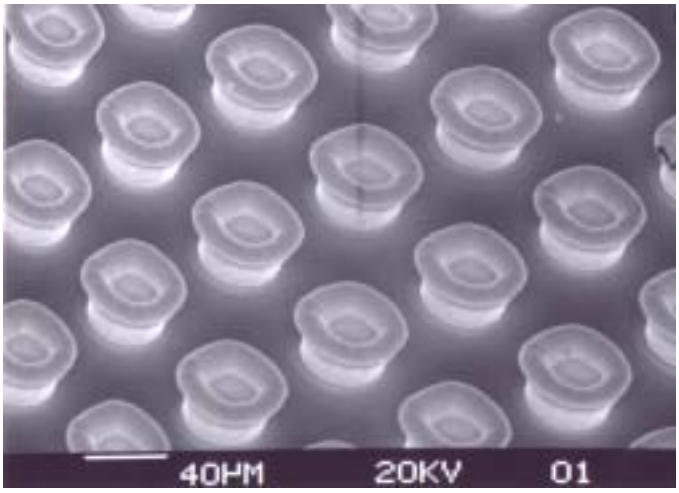

Figure 6. SEM image of an electrode with an array of hollow cylindrical structures.

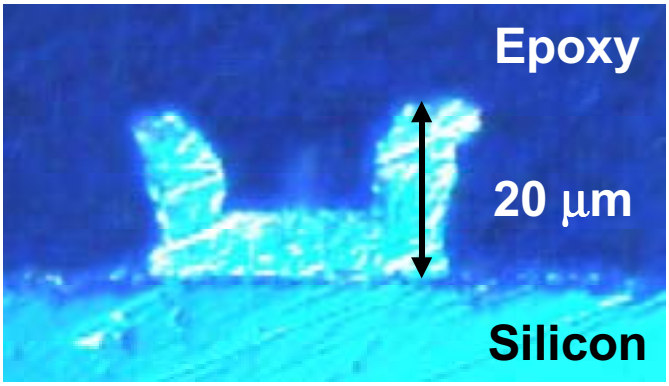

Figure 7. Cross section of a hollow cylindrical electrode. Note the equal thickness in the electrodeposit on the bottom surface (seed layer) and sidewalls (photoresist plating mold).

Thus proportionality between conductance and surface area is observed in our experimental impedance measurements. From the impedance curve of each electrode sample, the value is taken at 1 kHz and plotted against the estimated surface area. For structures with an aspect ratio of $h/w = 1$, a doubling of the effective electrode conductance is expected and observed (Fig. 9a). However, when the aspect ratio is

increased further to realize a larger surface area, experimental results show that the improvement in conductance advantage plateaus at a four-fold increase in physical surface area (fig. 9b). The abnormally high conductance for the first few samples can be due to errors in surface area calculation. Since the plateau can be overcome by switching to a more conductive solution, this indicates that the measured conductance is limited by the electrolyte resistance R_s in the high-aspect ratio features.

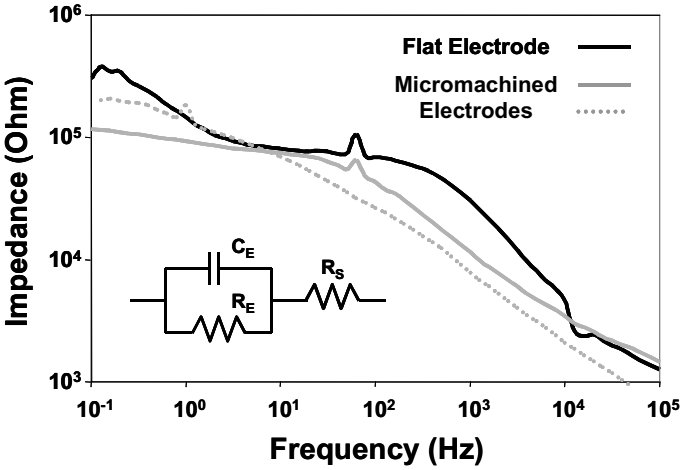

Plot of electrode-electrolyte impedance as a function of electrode frequency. Inset is a linear circuit analogue of the electrical characteristics of the electrode-electrolyte interface.

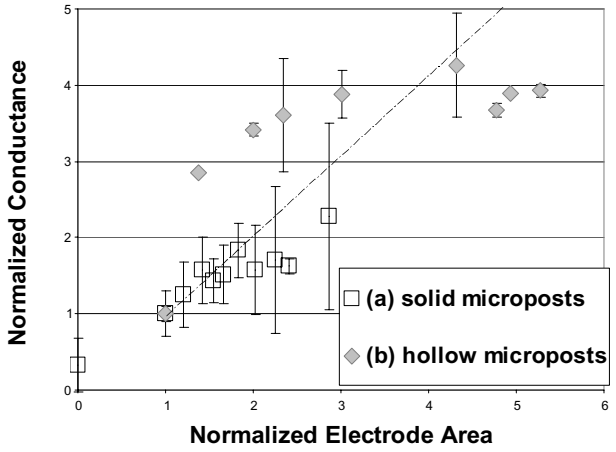

Figure 8. Plot of electrode conductance as a function of calculated electrode surface area, normalized with respect to the flat electrode.

III. CONCLUSION

The need for retinal prosthetic systems to have a high stimulation resolution drives the development of increasingly dense microelectrode arrays. The trade off between electrode size and the charge injection limit of electrode metals can be improved by using micromachining techniques to increase the effective surface area of the electrode in a stable fashion. A batch fabrication process has been developed to integrate arrays of Pt or Au microelectrodes in the shape of solid microposts to increase the surface area. A unique fabrication process has also been developed that enables the doubling of the surface enhancement provided by microtexturing the electrode surface. Specifically, an incomplete rinse after development enables the sidewalls of the photoresist plating mold to be conductive enough to act like an extension of the seed layer and the result are hollow microposts. Experimental measurements indicate that increasing the aspect ratio of the microposts does increase the effective area of the electrode asymptotically to a value approximately four times larger. By micromachining the electrodes of a retinal prosthetic in a similar way it should be possible to achieve a higher stimulation and hence visualization resolution.

ACKNOWLEDGMENT

The authors thank Nick Talbot at Second Sight, LLC for his guidance in aspects of the fabrication process. This work was supported by NIH / NEI contract 1 R24 EY12893-02. The corresponding author is Jack W. Judy. He may be contacted at 68-121 Engineering IV, 420 Westwood Plaza, Los Angeles, CA, 90095-1594, tel: (310) 206-1371, fax: (310) 861-5055, and email: jjudy@ee.ucla.edu. Other authors may be contacted via email: Andy Hung (ahung@ee.ucla.edu), and David Zhou (dmzhou@2-sight.com), Robert Greenberg (bob@2-sight.com).

REFERENCE:

[1] H. Thielecke, T. Stieglitz, H. Beutel, T. Matthies, H. H. Ruf, and J. U. Meyer, "Fast and precise positioning of single cells on planar electrode substrates," *IEEE Eng Med.Biol.Mag.*, vol. 18, no. 6, pp. 48-52, Nov.1999.

[2] K. L. Drake, K. D. Wise, J. Farraye, D. J. Anderson, and S. L. BeMent, "Performance of planar multisite microprobes in recording extracellular single-unit intracortical activity," *IEEE Trans.Biomed.Eng*, vol. 35, no. 9, pp. 719-732, Sept.1988.

[3] G. T. Kovacs, C. W. Storment, M. Halks-Miller, C. R. Belczynski, Jr., C. C. Della Santina, E. R. Lewis, and N. I. Maluf, "Silicon-substrate microelectrode arrays for parallel recording of neural activity in peripheral and cranial nerves," *IEEE Transactions on Biomedical Engineering*, vol. 41, no. 6, pp. 567-577, June1994.

[4] Q. Bai and K. D. Wise, "Single-unit neural recording with active microelectrode arrays," *IEEE Trans.Biomed.Eng*, vol. 48, no. 8, pp. 911-920, Aug.2001.

[5] M. S. Humayun, E. de Juan Jr, J. D. Weiland, G. Dagnelie, S. Katona, R. Greenberg, and S. Suzuki, "Pattern electrical stimulation of the human retina," *Vision Research*, vol. 39, no. 15, pp. 2569-2576, July1999.

[6] M. S. Humayun, E. de Juan Jr, G. Dagnelie, R. J. Greenberg, R. H. Propst, and D. H. Phillips, "Visual perception elicited by electrical stimulation of retina in blind humans," *Arch.Ophthalmol.*, vol. 114, no. 1, pp. 40-46, Jan.1996.

[7] W. Liu, E. McGucken, K. Vichienchom, S. M. Clements, S. C. DeMarco, M. Humayun, E. De Juan, J. Weiland, R. Greenberg, "Retinal prosthesis to aid the visually impaired," *IEEE Int. Conf. Systems, Man, and Cybernetics, Tokyo,* vol. 4, p. 364-9. 1999.

[8] G. S. Brindley, *Physiology of the retina and visual pathway*, 2d ed ed. Baltimore: Williams & Wilkins, 1970.

[9] A. J. Bard, and L. R. Faulkner, *Electrochemical methods, fundamentals and applications* New York: Wiley, 1980.